Available online at www.pelagiaresearchlibrary.com

Pelagia Research Library

Advances in Applied Science Research, 2014, 5(2):359-367

Pelagia Research Library

ISSN: 0976-8610
CODEN (USA): AASRFC

Numerical simulation of turbulent forced convection in a venturi channel with fully developed flow at the inlet

Serge Wendsida Igo[1], Kokou N'wuitcha[2], K. Palm[1], Lucian Mihaescu[3] and D. J. Bathiébo[4]

[1]*Institut de Recherche en Sciences Appliquées et Technologies (IRSAT/CNRST). Département Energie, 03 BP 7047 Ouagadougou 03, Burkina Faso*
[2]*GPTE-LES Département de Physique, Université de Lomé, BP 1515, Togo*
[3]*Polytechnic University of Bucharest (UPB), Department of Mechanical Engineering, Romania*
[4]*Laboratoire d'Energies Thermiques Renouvelables (LETRE), Université de Ouagadougou, 03 BP 7021 Ouagadougou 03, Burkina Faso*

ABSTRACT

In this work, a 2D turbulent forced convection air flow in a venturi channel has been numerically simulated using fluent. Transfers equations are described by the Reynolds Averaged Navier-Stokes equations (RANS) and the vicious model is the turbulent standard k-ε model. A fully-developed power-law profile is assumed for the inlet stream wise velocity. The results are presented as velocity field, static and dynamic pressures fields, streamlines field, vorticity and turbulent kinetic energy fields. They show that the region of maximum turbulent kinetic energy is the diffuser wall region extending to the channel exit and the turbulence shifts away from the diffuser wall in the flow direction.

Key words: venturi channel, turbulent flow, fully developed flow, CFD methods, fluent

---

INTRODUCTION

Venturi channels are widely used as scrubbers for particles and gaseous collection from industrial exhaust [1] or to meter gas flows [2]. These devices consist of channel with three parts : a convergent section, a throat and a divergent section or diffuser. Numerical turbulent studies in venturi channels are scarce because of the one hand, the complexity of the geometrical configuration and the other hand, the difficulty to model the turbulent flow along the venturi. Among the turbulence models in gas flow, the standard k-ε model [3] is the most popular. In many numerical studies in venturi channels, the velocity gas field is calculated using this model [4,5]. However, it is well know that near the walls occurs important vicious forces, so, the standard k-ε model which is suitable for large Reynolds numbers is no longer applicable. To solve this problem, two solutions can be used. The first solution consist to use the standard k-ε model with wall functions in order to force the first node of the computational grid to be in the sub-layer. The second solution consist to use directly the k-ε LRN (Low Reynolds Number) model [6]. The gas entry conditions are one of the simulation problems. It is rare in practice to encounter an uniform inlet flow into a venturi channel. Igo et al. studied the turbulent gas cleaning in a rectangular venturi scrubber using the k-ε LRN model with fully developed flow at the inlet and show that the turbulence is developing from the inlet to the outlet of the venturi channel [7]. Their CFD method was based on a mathematical transformation of the venturi wall and the finite volume method which has been implemented by Thomas and Gauss algorithms. Using a conical diffuser (Azad diffuser) which has a total divergence angle 8° and a fully developed flow at the inlet, Okwuobi and Azad [8] showed that the peak of the turbulent fluctuations shifts away from the wall along the streamwise direction of the flow. They also show that the rate of turbulent energy production reaches a maximum value at the edge of the wall layer. To facility the turbulent modeling and simulation in gas flow, CFD tools which include pre-processors, solvers and post-processors are more and more used. Among these tools, the solver post-processor fluent [9] and the pre-processor gambit [10] are widely used. Many studies based on these tools are widely been performed [11,12,13]. Recently, Igo et al. [14] studied the turbulent gas flow in a venturi channel using fluent and gambit. They showed

that the venturi effect is well predicted by the fluent code. Therefore, the objective of the present study is to extend this work and provide more results of turbulent flow in venturi channels.

PROBLEM FORMULATION

The venturi channel is composed of two iron plates of sections lengths (L_1, L_2, L_3). The inlet diameter is R_o and the throat diameter is R_{th}. The wall plates are subjected to a constant temperature T_w. A fully-developed turbulent air flow with average velocity U_e enters at the venturi channel with an uniform temperature T_e.

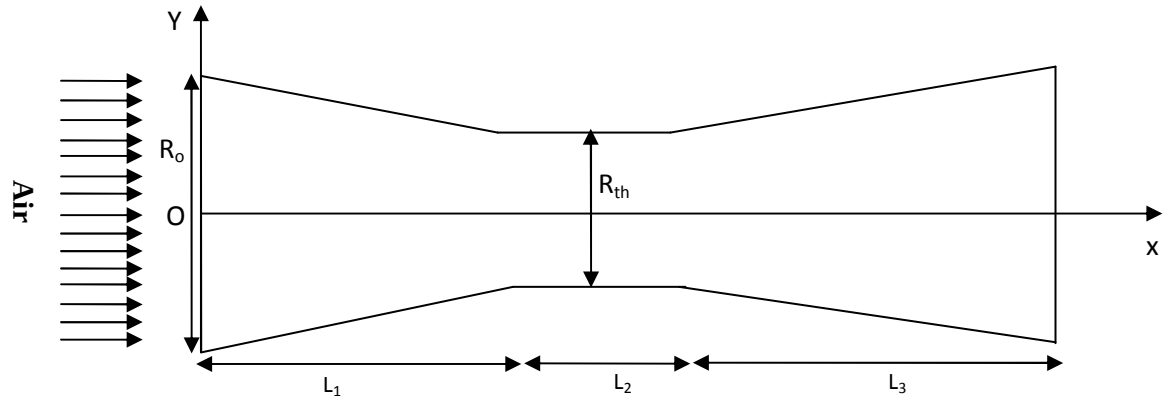

Fig 1. Schematic representation of the studied system in the (O,X,Y) referential

It is assumed that the flow is incompressible and the transfers are two-dimensional, axisymetric and steady state.

The RANS equations modeling the turbulent incompressible air flow through the venturi channel are:

-Continuity equation

$$\frac{\partial U_i}{\partial x_i} = 0 \tag{1}$$

-Momentum equation

$$\frac{\partial}{\partial x_j}\left(\rho U_i U_j\right) = -\frac{\partial P}{\partial x_i} + \frac{\partial}{\partial x_j}\left[\mu\left(\frac{\partial U_i}{\partial x_j} + \frac{\partial U_j}{\partial x_i}\right)\right] - \frac{\partial}{x_j}\left(\rho\overline{u_i u_j}\right) \tag{2}$$

U, P are respectively the average velocity and pressure, u is the velocity fluctuation.

The Reynolds stresses $\left(\rho\overline{u_i u_j}\right)$ is defined by the Boussinesq approximation:

$$\rho\overline{u_i u_j} = -\mu_t\left(\frac{\partial U_i}{\partial x_j} + \frac{\partial U_j}{\partial x_i}\right) + \frac{2}{3}\rho k\delta_{ij} \tag{3}$$

μ_t is the turbulent viscosity, k is the turbulent kinetic energy and δ is the Kronecker symbol.

To close these equations, the standard k-ε model equations are:

$$\frac{\partial}{\partial x_j}\left(\rho U_j k\right) = \frac{\partial}{\partial x_j}\left[\left(\mu + \frac{\mu_t}{\sigma_k}\right)\frac{\partial k}{\partial x_j}\right] + Q - \rho\varepsilon \tag{4}$$

$$\frac{\partial}{\partial x_j}\left(\rho U_j \varepsilon\right) = \frac{\partial}{\partial x_j}\left[\left(\mu + \frac{\mu_t}{\sigma_\varepsilon}\right)\frac{\partial \varepsilon}{\partial x_j}\right] + \left(C_{\varepsilon 1} Q - \rho C_{\varepsilon 2}\varepsilon\right)\frac{\varepsilon}{k} \tag{5}$$

$$\mu_t = \rho C_\mu \frac{k^2}{\varepsilon} \tag{6}$$

Q is the term of production and is defined by:

$$Q = \left[\mu_t \left(\frac{\partial U_i}{\partial x_j} + \frac{\partial U_j}{\partial x_i} \right) \right] \frac{\partial U_i}{\partial x_j} \tag{7}$$

$C_\mu = 0.09$; $\sigma_k = 1$; $\sigma_\varepsilon = 1.3$; $C_{\varepsilon 1} = 1.44$; $C_{\varepsilon 2} = 1.92$ are the constants of the k-ε model.

NUMERICAL SIMULATION

Mesh

The mesh is generated using the Gambit 2.2 software. Due to symmetry, only the half domain needs to be considered. The mesh size is very close near the walls to take account the turbulent boundary layer.

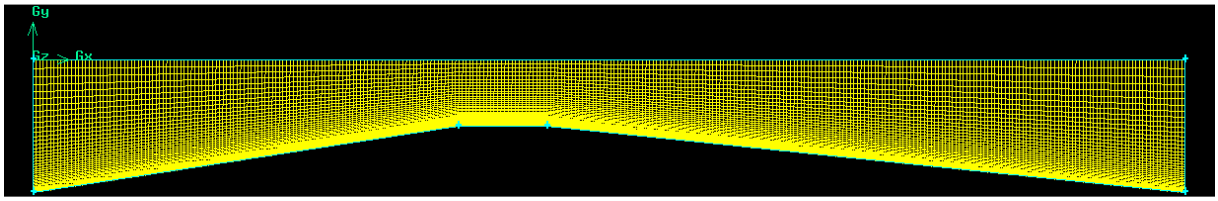

Fig 2. Channel mesh

Simulation

Transfer equations are solved using fluent 6.2, a computational fluid dynamics software which enables accurate simulation of flow in channels. The Standard Wall Function is used for the treatment of the turbulent boundary layer. To use this function, each wall-adjacent cell's centroid should be located within the log-law layer ($30 < y^+ < 300$).

In order to performed the simulation, the following boundaries conditions are considered:

-At the inlet

A fully-developed power-law profile (n=7) is assumed for the streamwise velocity. As we consider the lower half channel, the inlet velocity profile is:

$$U = U_o \left(1 + \frac{y}{R_o} \right)^{1/n}$$

U_o is the centerline velocity.

$$U_o = U_e \frac{(2n+1)(n+1)}{2n^2}$$

U_e is the average inlet velocity which is correlated to the inlet Reynolds number Re.

$$Re = \frac{U_e Dh}{\upsilon_e}$$

Dh is the hydraulic diameter and υ_e the air inlet cinematic viscosity.

The computing of the inlet velocity profil is performed by using the fluent 2D UDF code.

The inlet turbulent kinetic energy k_e and his rate of dissipation ε_e can be expressed as:

$$k_e = \frac{3}{2}(I_e U_e)^2$$

$$\varepsilon_e = C_\mu^{3/4}(k_e)^{3/2}/l$$

I_e is the inlet turbulence rate and l the turbulence scale:

$I_e = 0.16(\mathrm{Re})^{-1/8}$ for internal fully developed flows.

l=0.07Dh

-At the walls : $T=T_w$ and the no-slip conditions are applied for the flow.

-At the symmetry axis : symmetry boundary condition is imposed.

-At the outlet : outflow boundary condition is imposed.

RESULTS AND DISCUSSION

In the present study, simulations were performed for R_o=0.3m, R_{th}=0.15m, L_1=0.48m, L_2=0.1m, L_3=0.72m, U_e=13 ms^{-1}, $T_e = T_w = 300K$.

Before print the results, we verify that the mesh is conform to the standard wall function law.

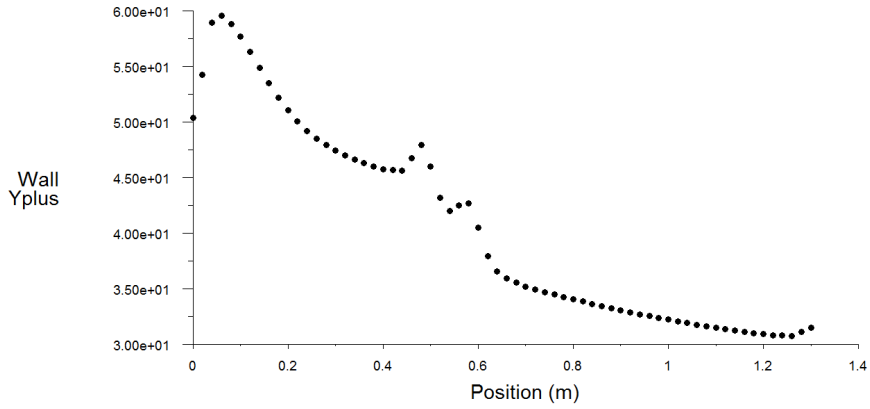

Fig 3. Wall Yplus evolution along the venturi channel

Wall Yplus (figure 3) is between 30 and 60. The mesh is conform to the standard wall function law.

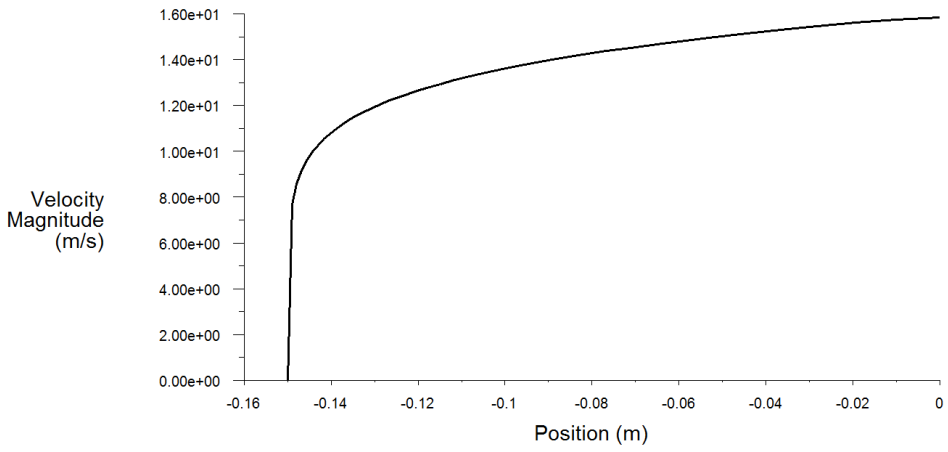

Fig 4. Inlet velocity

Figure 4 shows the inlet velocity computed using the fluent 2D UDF code. As seen, the inlet velocity profile is turbulent fully-developed and is an agreement with our hypothesis.

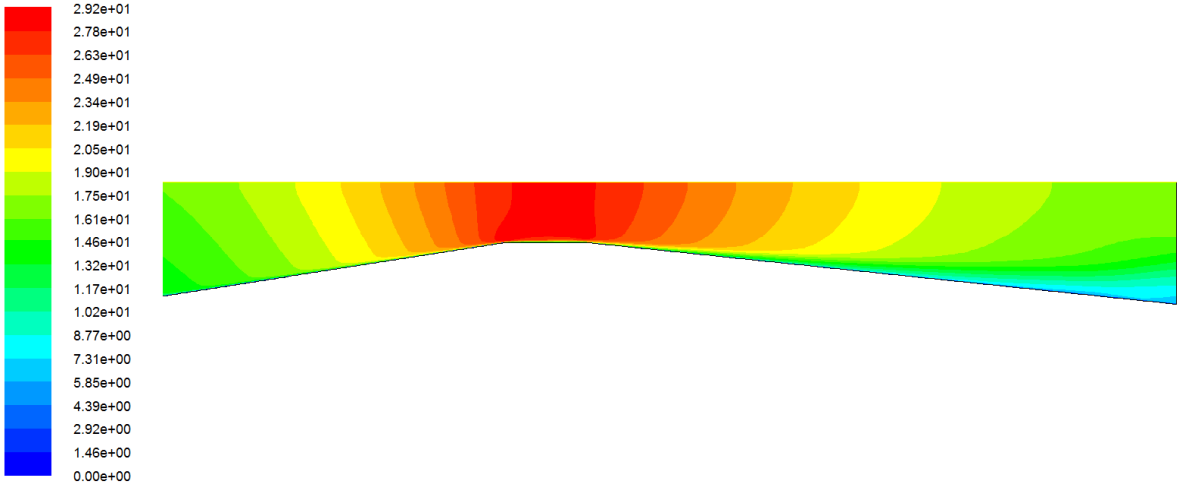

Fig 5. Contours of velocity magnitude (m/s)

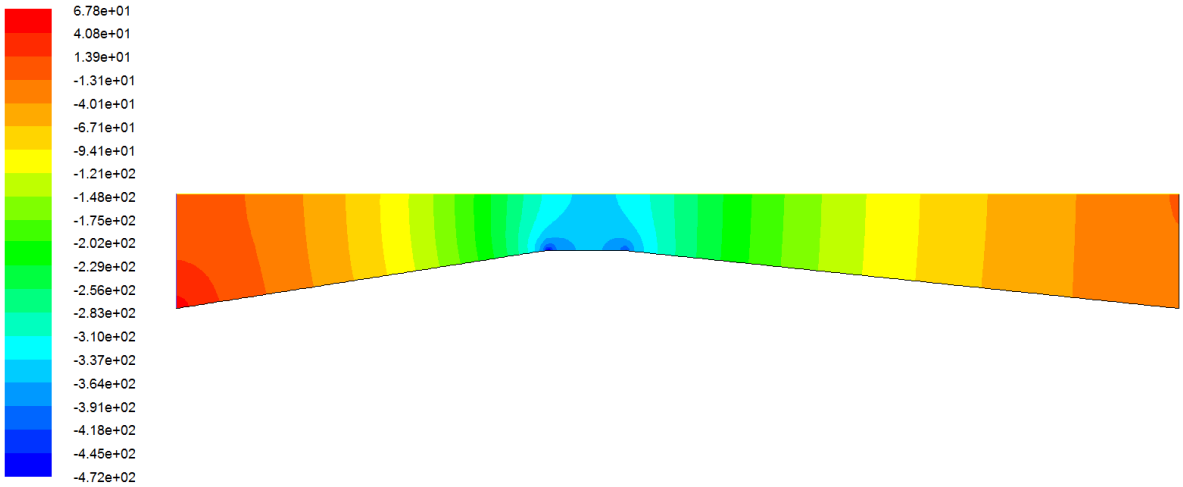

Fig 6. Contours of static pressure (Pascal)

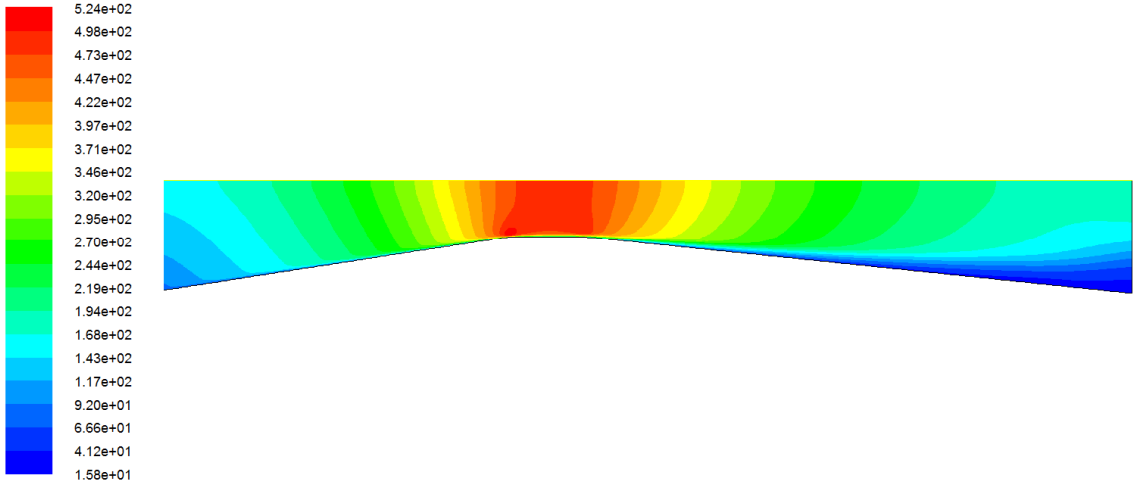

Fig 7. Contours of dynamic pressure (Pascal)

Figures 5-6 show respectively the velocity and the static pressure fields in the venturi. We note that the flow velocity increases as the flow moves in the converging section to reach a maximum value at the venturi throat. In fact, in the converging section, there is a continuous increase of the pressure drop due to the acceleration of the air velocity resulting of the conversion of the air potential energy into kinetic one. According to the flow rate conservation law

and considering the venturi diameter ratio (R_{th}/R_o) equal to 0.5, the velocity must double in the throat and we can note it on Figure 5. In the diverging section, the decrease of the velocity is due to the expansion of the channel diameter. The evolution of the static pressure along the venturi is the opposite of the velocity one. The lowest pressures are observed in the throat. The large depressions seen at the throat corners are due to the change of the flow direction. The flow in the venturi channel and is then an agreement with the Bernoulli law : this is venturi effect.

Figure 7 shows the dynamic pressure field. The dynamic pressure is by definition proportional to the square of the velocity. We indeed notice that the dynamic pressure and the velocity have approximately the same evolution in the channel. The dynamic pressure increases from the inlet to the throat and decreases from the throat to the outlet. The highest values are observed in the venturi throat.

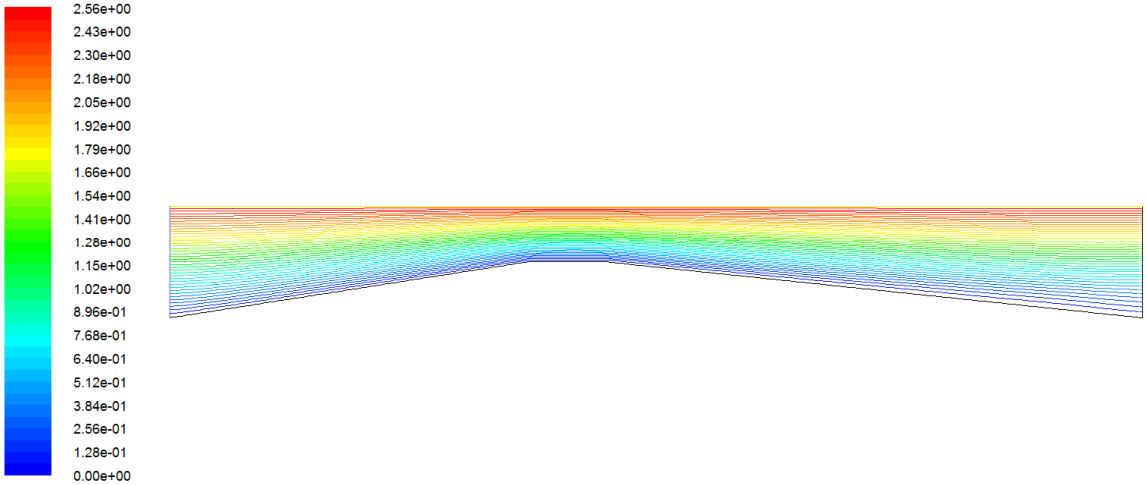

Fig 8. Contours of stream function (Kg/s)

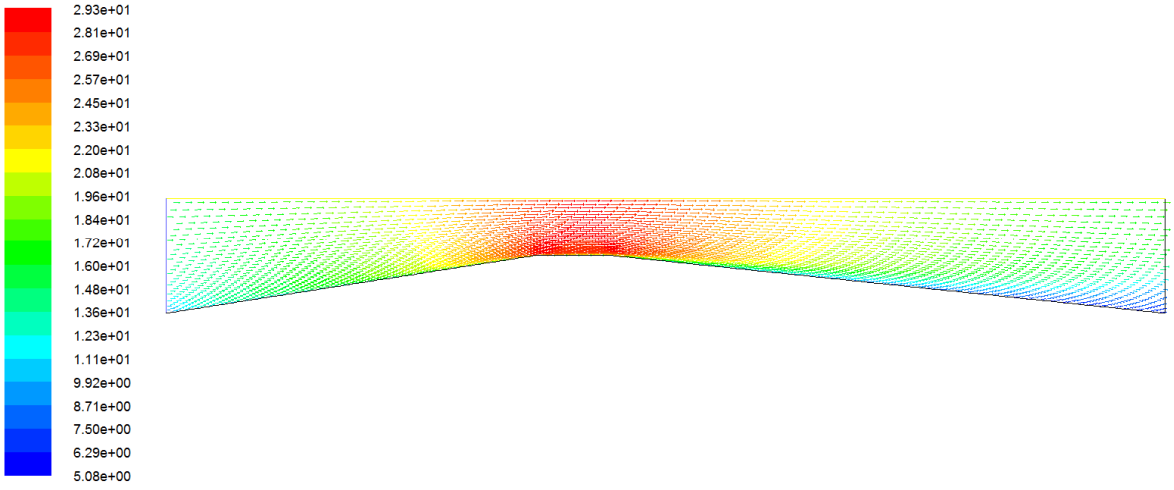

Fig 9. Channel velocity vectors colored by velocity magnitude (m/s)

Figures 8-9-10 illustrate the flow structure, respectively the streamlines field, the channel velocity vectors field and the diffuser velocity vectors field. We note that streamlines (figure 8) are very close in the convergent section and they are merged in the throat due to the reduction of the channel section and the augmentation of the velocity. In the divergent section, the streamlines are detached from the wall particularly at the channel exit. The streamlines evolution in the channel shows that the flow is non-separated because the channel divergence angle (about 6°) and the diffuser aspect ratio (0.72/0.15=4.8) are low. According to the diagram of typical flow regions [15], these geometrical parameters cannot create a separated flow in the channel. The observation of the velocity vectors (figure 9) shows that the flow moves from the channel inlet to the channel outlet, but we can see the change of velocity vectors (figure 10) whose movements become very random in the diffuser wall region. This situation is typical in the diffusers and is due to a retarded flow (adverse pressure gradient) which appears in this kind of channel. And it is well know that this phenomenon contribute to amplify the velocity fluctuations.

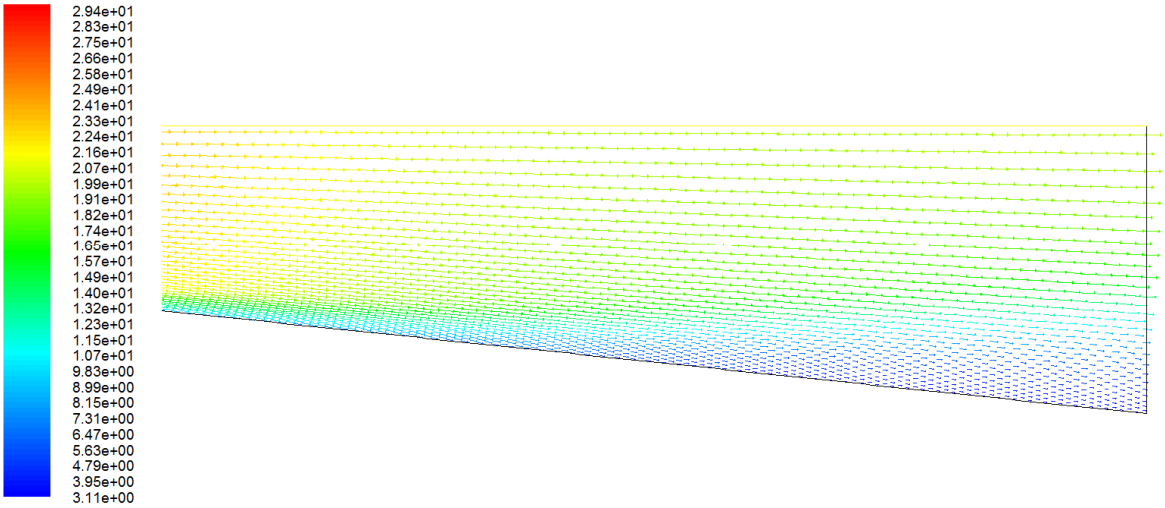

Fig 10. Diffuser velocity vectors colored by velocity magnitude (m/s)

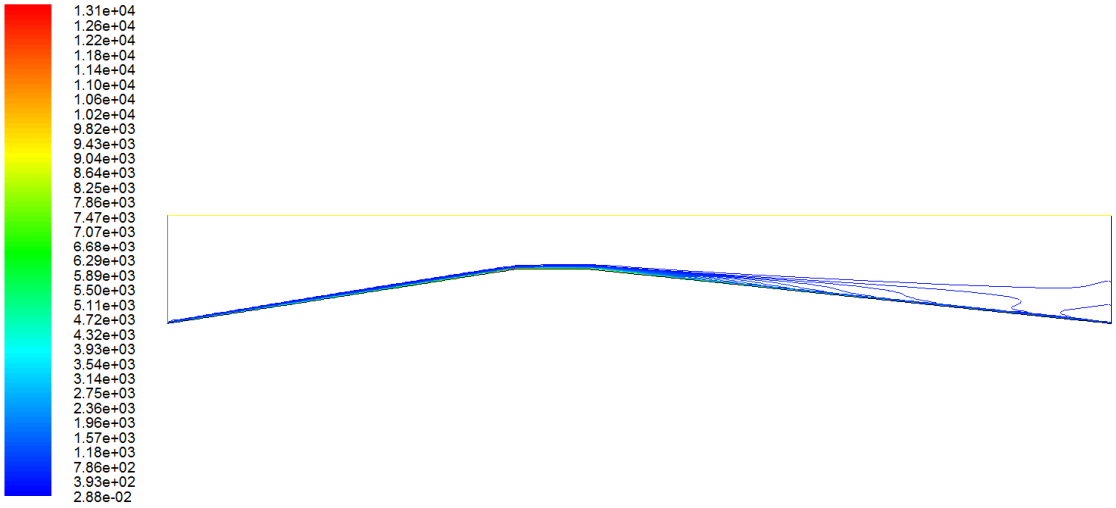

Fig 11. Contours of vorticity magnitude (1/s)

figure 11 shows the contours of the vorticity magnitude. We note that some low amplitude vortices appear in the diffuser wall region extending to the channel exit. This result corroborate the previous one. In fact, it is well know that a vortices zone is an important region of velocity fluctuations.

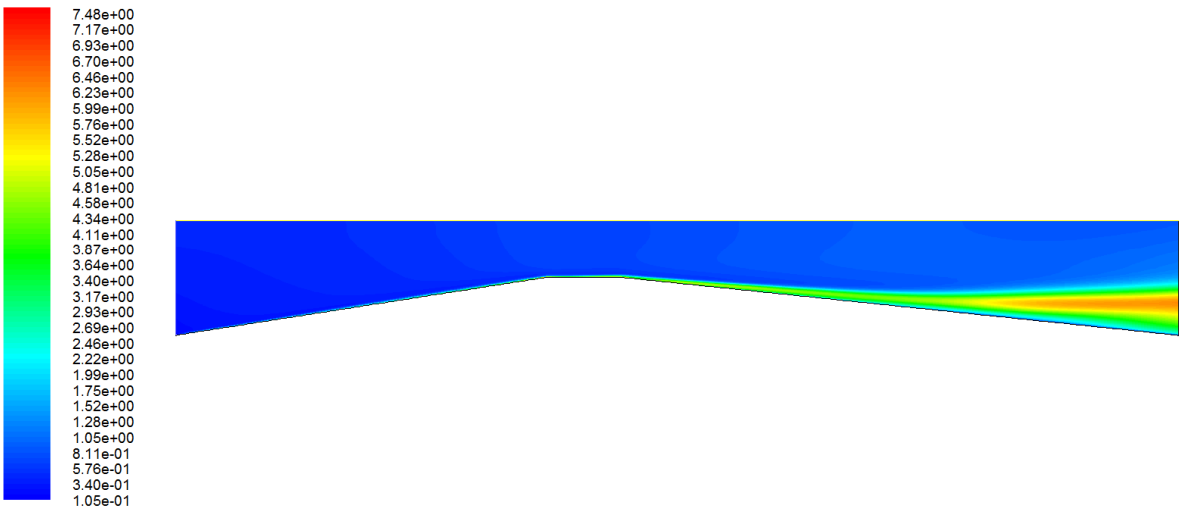

Fig 12. Contours of turbulent kinetic energy (k) (m^2/s^2)

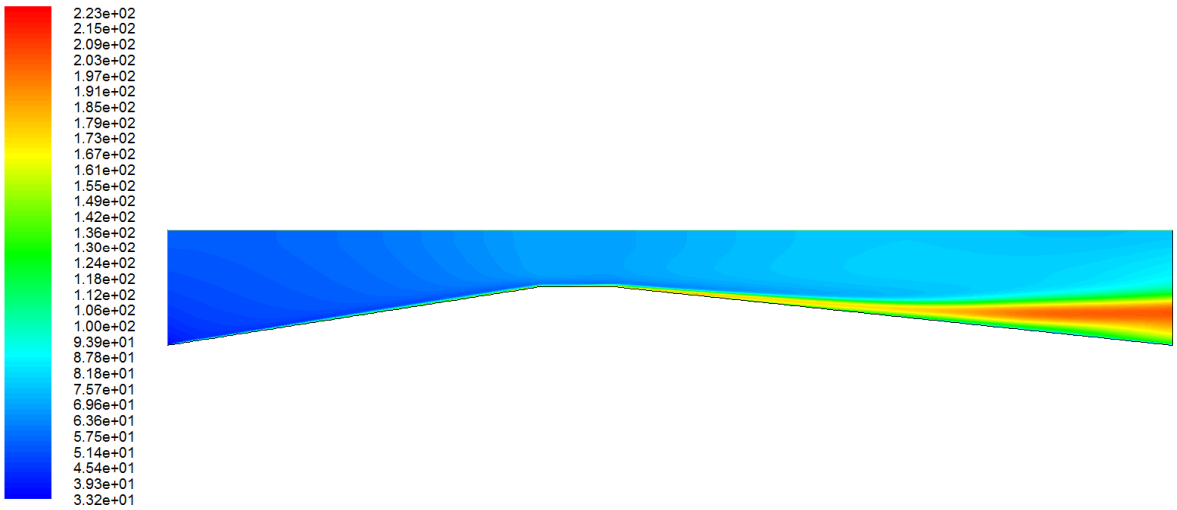

Fig 13. Contours of turbulent intensity (%)

Figures 12-13 show the contours of the turbulence intensity and the turbulent kinetic energy respectively. We note that the turbulent kinetic energy and the turbulence intensity have approximately the same evolution and their maximum values are observed in the diffuser wall region extending to the channel exit. This result is the consequence of the two previous results. In a channel, the turbulence intensity is of course improved in the zones where the velocity fluctuations are important, and this zone for the studied channel is the diffuser wall region extending to the channel exit. We observe also that the turbulence shifts away from the wall in the flow direction.

CONCLUSION

A forced turbulent convection air flow in a 2D venturi channel was numerically investigated in the present study using fluent. A fully-developed power-law profile is assumed for the inlet streamwise velocity. Transfers equations are described by the Reynolds Averaged Navier-Stokes equations and the vicious model is the turbulent standard k-ε model. The major results are:

-The venturi effect is well predicted.
-The high velocity fluctuations zone is the diffuser wall region extending to the channel exit.
-The turbulence is very important in the diffuser wall region extending to the channel exit and shifts away from the diffuser wall in the flow direction.

Acknowledgements
The authors thank the AUF (Agence Universitaire de la Francophonie) for his financial support. They also thank the Polytechnic University of Bucharest (UPB) for his technical support.

REFERENCES

[1] R.H. Boll, *Industrial and Engineering Chemistry Fundamentals*,**1973**,12, 40-50.
[2] W. Jitschin, M. Ronzheimer, S. Khodabakhshi, *Vacuum*, **1999**, 53, 181-185.
[3] B.E. Launder, D.B. Spalding; Mathematical models of turbulence, academic press, London, **1972**.
[4] S.I. Pak, K.S. Chang, *Journal of Hazardous Material*, **2006**, 138, 560-573.
[5] F. Ahmadvand, M.R. Talaie, *Chemical Engineering Journal*, **2010**, 160, 423–431.
[6] B.E. Launder, B.I. Sharma, *Letters in heat and mass transfer*, **1974**, 1, 131-138.
[7] S.W. Igo, PhD thesis, Ouagadougou University (Ouagadougou, BF, **2011**)
[8] Fluent Inc; Fluent 6.2 tutorial Guide, Lebanon, NH, **2004**.
[9] Fluent Inc; Gambit 2.2 tutorial Guide, Lebanon, NH, **2004**.
[10] A. Majid, Q.Y. Chang, N.S. Zhong, J.W. Jian, R. Athar, *Applied Mechanics and Materials*, **2012**, 3630-3634.
[11] G.G. Vádila, B. Rodrigo, A.S.G. José, R.C. José, *Industrial and Engineering Chemistry Research*, **2012**, 51, 8049–8060.
[12] A. Majid, Y. Changqi, S. Zhongning, W. Jianjun, G. Haifeng, *Nuclear Engineering and Design*, **2013**, 256, 169-177.
[13] P.A.C. Okwuobi, R.S. Azad, *journal of fluids mechanics*, **1973**, 57, 603-622
[14] S.W. Igo, M. Lucian, P. Tudor, 2nd International conference of thermal equipment, renewable energy and rural

development, 20-22 June **2013**, Baile Olanesti Romania (TE-RE-RD 2013, Romania) 51-54.
[15] F.M White; Fluids mechanic,3rd edition, McGraw-Hill, Inc., New York, **1994**.